Journal of Materials Chemistry A

PAPER

View Article Online
View Journal | View Issue

Cite this: J. Mater. Chem. A, 2014, 2, 345

Received 23rd September 2013
Accepted 16th October 2013

DOI: 10.1039/c3ta13818f

www.rsc.org/MaterialsA

Quasi-solid-state, coaxial, fiber-shaped dye-sensitized solar cells†

Hao Sun, Houpu Li, Xiao You, Zhibin Yang, Jue Deng, Longbin Qiu and Huisheng Peng*

A quasi-solid-state, coaxial, fiber-shaped dye-sensitized solar cell is developed by wrapping transparent and conducting carbon nanotube sheets on a modified Ti wire. The use of eutectic melts and design of the coaxial structure enable effective contacts between the two electrodes and active layer with a good performance, including high thermal stability and flexibility.

Introduction

Dye-sensitized solar cells (DSCs) have attracted increasing attention in recent years due to many promising advantages.[1–6] For instance, the capability of being flexible enables applications that are impossible to achieve for conventional silicon-based technologies, such as various portable electronic devices, and well meet the mainstream development in modern electronics. Flexible DSCs are mostly explored due to the advantages of low cost and facile fabrication.[7–12] However, liquid electrolytes are generally used to fabricate flexible DSCs which need to be sealed with complex processes. In addition, liquid electrolyte may leak under bending, which severely limits the stability and lifetime of flexible DSCs.[13–15] Furthermore, the operation temperature often exceeds 70 °C in daily applications, or even 100 °C in some fields such as use in spacecrafts, while most liquid electrolytes evaporate and cannot survive during use.

On the other hand, flexible DSCs typically appear in a planar format that cannot satisfy many integrated and portable devices and facilities that also require a small size and light weight.[16] Some attempts have been recently made to fabricate flexible DSCs by twisting two fiber electrodes into a wire format.[17,18] However, compared with the planar structure, the use of liquid electrolytes proves to be much more difficult for the sealing of long and flexible wire-shaped DSCs. Two twisted fiber electrodes have also been found to be disassembled from each other under bending or other deformations, so the twisted DSCs show a limited stability as flexible devices. Recently, some attempts have been made to fabricate coaxial photovoltaic fibers to improve the mechanical stability. Weintraub and co-workers developed a coaxial DSC fiber with a maximal efficiency of 0.44% by using a ZnO nanowire array, Pt film, and liquid electrolyte as the working electrode, counter electrode, and electrolyte, respectively.[19] Bae and co-workers further modified the above fiber DSC by replacing the conventional Pt with graphene, although the energy conversion efficiency was relatively lower (0.02%).[20] To further increase the energy conversion efficiency, Zhang and co-workers introduced a randomly dispersed carbon nanotube membrane as the counter electrode, and a maximal efficiency of 1.6% was achieved.[13] It has been well recognized that the randomly dispersed carbon nanotubes produce network structures, so the charges had to transport among a lot of boundaries with low efficiencies.[21] In addition, the use of liquid electrolytes has proved to be difficult to seal the resulting fiber DSCs, and they also showed a relatively low thermal stability.

Here we have developed a quasi-solid-state, coaxial, fiber-shaped DSC which has simultaneously overcome the above challenges (Fig. 1). A modified Ti wire serves as a working electrode that is coated with photoactive components and a quasi-solid-state electrolyte, and a transparent and conducting multi-walled carbon nanotube (MWCNT) sheet is then uniformly wound on the outer surface as the counter electrode. This coaxial structure enables an effective contact area for a low electrical resistance and a high stability. The winding of an aligned MWCNT sheet that is mechanically and thermally stable further greatly improves the cell stability.

Experimental section

The synthesis details of the spinnable MWCNT arrays and eutectic melts are described in the ESI.† An electrochemical anodization was used to grow aligned titania nanotubes on a Ti wire with a diameter of 127 μm.[24] The growth occurred with a 0.3 wt% NH_4F/8 wt% H_2O/ethylene glycol solution as the electrolyte and voltage of 60 V in a two-electrode electrochemical cell with a Ti wire and Pt sheet as the anode and cathode, respectively. The lengths of titania nanotubes were controlled by varying the oxidation time, *i.e.*, 2 h for 10 μm, 4 h for 22 μm,

State Key Laboratory of Molecular Engineering of Polymers, Department of Macromolecular Science, and Laboratory of Advanced Materials, Fudan University, Shanghai 200438, China. E-mail: penghs@fudan.edu.cn

† Electronic supplementary information (ESI) available. See DOI: 10.1039/c3ta13818f

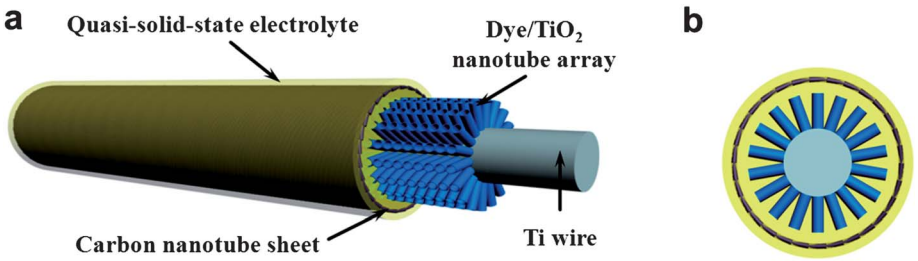

Fig. 1 Schematic illustration of the quasi-solid-state, coaxial, fiber-shaped DSC. (a) Side view. (b) Cross-sectional view.

6 h for 32 μm, and 8 h for 40 μm. The resulting wires were immersed in deionized water to remove the residual electrolyte, followed by heating at 500 °C for 1 h and annealed in air.

To fabricate the quasi-solid-state, coaxial photovoltaic fiber, the titania nanotube-modified Ti wire was immersed in a 40 mM $TiCl_4$ aqueous solution. After the treatment at 70 °C for 30 min, the resulting wire was rinsed with deionized water, followed by annealing at 450 °C for 30 min in air. When the temperature was cooled to 120 °C, it was immersed in 0.3 mM N719 solution (a solvent mixture of dehydrated acetonitrile and *tert*-butanol with a volume ratio of 1/1) for 16 h, when a high absorption of the N719 dye onto TiO_2 nanotubes was achieved. The MWCNT sheet was pulled out of a spinnable CNT array with a razor blade and then carefully wrapped onto the modified Ti wire. Photovoltaic fibers with different thicknesses of MWCNT sheets were realized by repeating the wrapping process above. A TiO_2 shell (~1 nm) was deposited on the TiO_2 nanotube array after the $TiCl_4$ treatment, which lowered the acceptor levels in TiO_2 in energy with improved injection efficiency, increased the roughness to absorb more dye molecules, and enhanced the electron lifetime with increased electron diffusion length. For convenience in the operation, the coaxial photovoltaic fibers could be transferred to a transparent flexible fluorinated ethylene propylene tube (diameter of 500 nm, Shanghai Yi Chuan Shui Plastic Products Co.), followed by a rapid injection of the melted electrolyte under heating at ~120 °C and sealing at both ends of the tube. During the measurement, the incident light was irradiated on the fiber-shaped DSC from the top in a direction perpendicular to the substrate.

Results and discussion

In this work, eutectic melts of 1-ethyl-3-methylimidazolium iodide (EMII), ionic liquid of 1-propyl-3-methylimidazolium iodide (PMII), and iodine was mixed and used as the quasi-solid-state electrolyte (Fig. S1†).[22] Imidazole-like cation is chemisorbed on the surface of working electrode to form a stable Helmholtz-like layer, which prevents the contact of I_3^- ions with the working electrode and inhibits the recombination of I_3^- ions and electrons in the titania conducting band. As a result, the fill factor and energy conversion efficiency can be increased in the DSC.[23] PMII was chosen as a component to improve the ion conductivity and offer I^- ions. As designed, the resulting electrolyte remains solid under 50 °C (Fig. S2 and S3†).

Perpendicularly aligned titania nanotubes were grown on a Ti wire by the electrochemical anodization.[24] Fig. 2a and b compare a Ti wire before and after the growth of the titania nanotubes, and it is uniform in diameter for both cases. Fig. 2d further shows a high magnification scanning electron microscopy image of titania nanotubes from a side view, and they are highly aligned and perpendicular to the Ti surface. Therefore, these titania nanotubes share the same length that is important for a uniform structure in the photovoltaic fiber. The diameter of the resulting core-sheath wire was increased to 155 μm from 127 μm of the original bare Ti wire. As the core Ti part shows a diameter of 91 μm, the length of the titania nanotubes can be calculated as 32 μm. Fig. 2d also shows that the titania nanotubes are uniform in diameter, with an inner diameter of ~80 nm and wall thickness of ~20 nm. The dye of N719 and electrolyte can then be coated onto the titania nanotubes. The MWCNT sheet with a thickness of ~20 nm is typically dry-drawn from the MWCNT arrays synthesized by chemical vapor deposition (Fig. S4a and Video S1†). The MWCNT sheet could be transparent with a transmittance over 88% (Fig. S4b†). The MWCNTs are highly aligned along the drawing direction to exhibit a high mechanical strength at the level of 10^2 to 10^3 MPa and electrical conductivities on the order of 10^2 to 10^3 S cm^{-1} (Fig. S5†).[25] The combined remarkable properties provide them

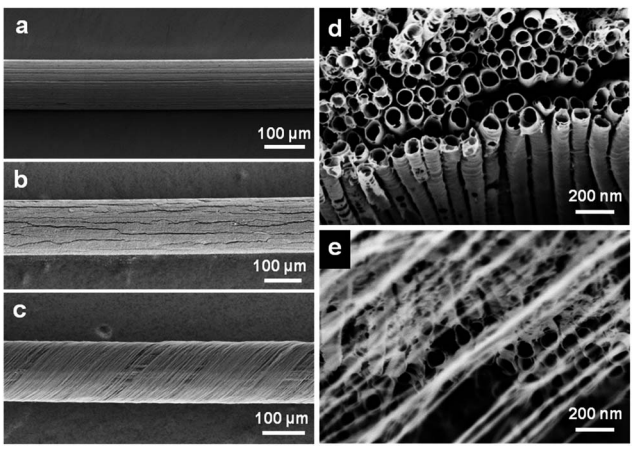

Fig. 2 Scanning electron microscopy (SEM) images of the coaxial DSC fiber. (a) A bare Ti wire. (b) Vertically aligned titania nanotubes grown on the Ti wire. (c) A single layer of highly aligned MWCNT sheet wrapped on (b). (d) Higher magnification of (b). (e) Higher magnification of (c).

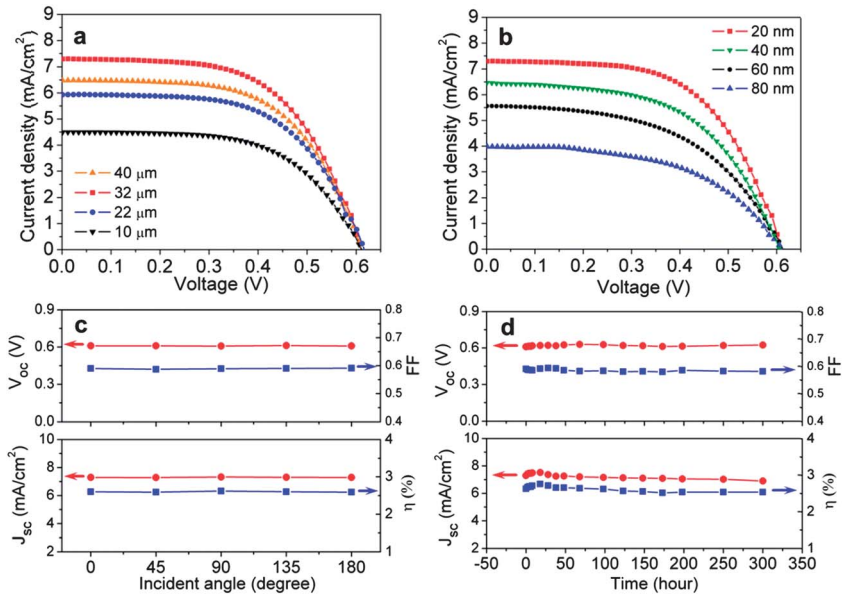

Fig. 3 *J–V* curves of the quasi-solid-state, coaxial DSC fiber. (a) Titania nanotubes with different lengths. (b) MWCNT sheets with different thicknesses. (c) Dependence of the photovoltaic parameters on the incident angle. (d) Changes of photovoltaic parameters during a period of 300 hours.

with promising applications as electrode materials in photovoltaic devices. Here the MWCNT sheet is stably wrapped on the titania nanotube-modified Ti wire as the counter electrode (Fig. 2c). The highly aligned structure of the MWCNTs in the sheet has been well maintained in the fiber-shaped device (Fig. 2e and S6†).

To optimize the coaxial photovoltaic fiber, titania nanotubes with different lengths and MWCNT sheets with different thicknesses have been used for a series of coaxial photovoltaic fibers. The lengths of titania nanotubes are controlled by varying the time of electrochemical anodization, and four increasing lengths of 10, 22, 32, 40 μm have been mainly studied. As generally accepted, the effective area of a fiber-shaped DSC was calculated by multiplying the length and diameter of the working electrode.[12,19,26–28] Fig. 3a compares the *J–V* curves of the resulting photovoltaic fibers under the same conditions. With the increasing length of titania nanotubes from 10 to 40 μm, the open circuit voltage (V_{oc}) and fill factor (FF) are maintained to be appropriately 0.61 V and 0.59, respectively. However, the short circuit current density (J_{sc}) is largely enhanced from 4.54 to 7.29 mA cm^{-2} with an increasing length from 10 to 32 μm and then decreased to 6.49 mA cm^{-2} with the further increase to 40 μm. The highest energy conversion efficiency of 2.6% appears at the length of ~32 μm. The increased J_{sc} may be explained by the fact that longer titania nanotubes absorb more dye, so more photoelectrons are excited under the same illumination. With the further increase of the length to exceed the penetration length of photons and diffusion length of electrons (*i.e.*, 32 μm in this work), the charge recombination becomes dominating to reduce the collecting efficiency of electrons.[29]

Photovoltaic fibers using the same length of TiO_2 nanotube arrays (32 μm) but different thicknesses of MWCNT sheets, *i.e.*, 20, 40, 60 and 80 nm have been compared. Fig. 3b shows representative *J–V* curves. With the increasing thickness from 20 to 80 nm, the V_{oc} remains almost unchanged at ~0.61, while both J_{sc} and FF are monotonically decreased. The decreased J_{sc} is explained by the fact that the incident light first penetrates the outer MWCNT sheet to reach the dye, although the penetrated light decreases with the increasing thickness of the MWCNT sheets. Accordingly, the generated photoelectrons are reduced to decrease the J_{sc} value. The transmittance is largely decreased with the increasing thickness of the MWCNT sheets. The decreased FF is mainly caused by the increased resistance of thicker MWCNT sheets. The resistances of aligned MWCNT sheets are dominated by the contact resistances among the MWCNTs as the resistances of individual MWCNTs are much lower, and thicker MWCNT sheets with the same number density have more boundaries with higher contact resistances.

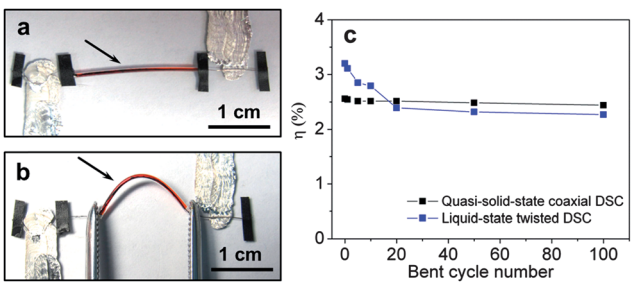

Fig. 4 (a and b) Photographs of a quasi-solid-state coaxial DSC fiber before and after bending. The two arrows show the DSC fiber. (c) The dependence of the energy conversion efficiency on the bent cycle number. The black and blue dots correspond to the quasi-solid-state coaxial DSC fiber and liquid-state twisted DSC wire, respectively. The liquid-state twisted DSC used the same amount of CNT as the quasi-solid-state coaxial DSC.

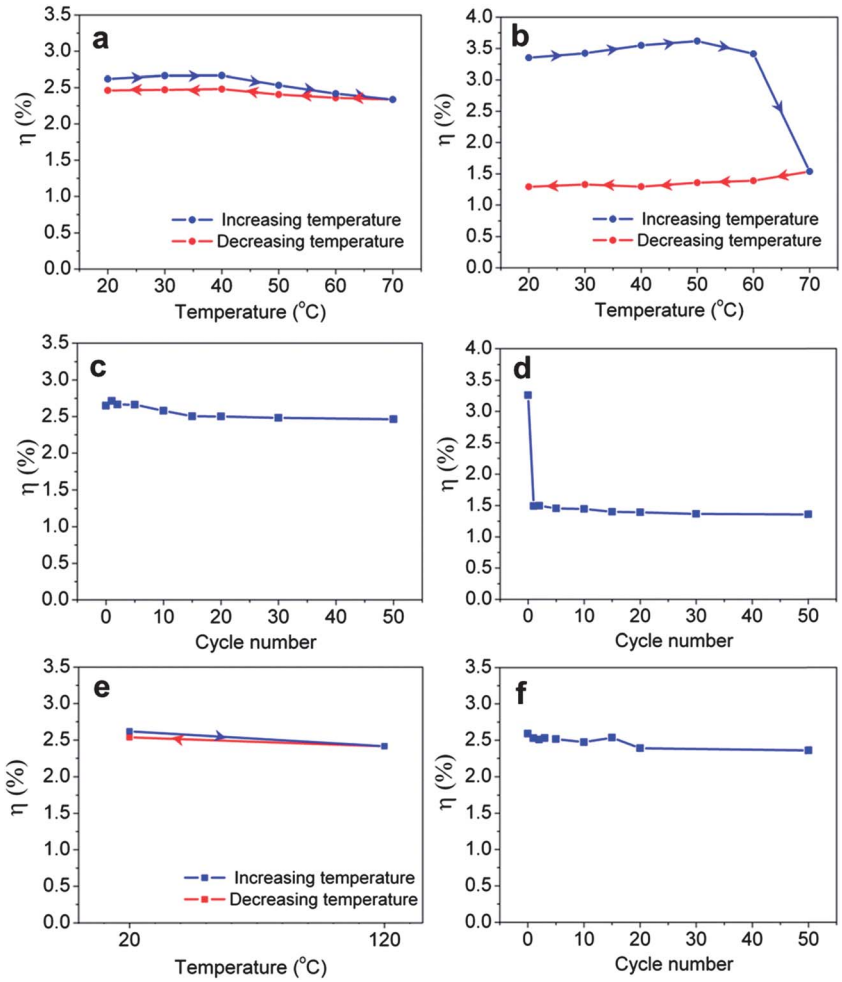

Fig. 5 Thermal stability of the quasi-solid-state coaxial DSC fiber and liquid-state twisted DSC wire. (a and b) Dependence of the energy conversion efficiency on the temperature for the quasi-solid-state coaxial DSC fiber and liquid-state twisted DSC wire, respectively. (c and d) Dependence of the efficiency on the cycle number for the quasi-solid-state coaxial DSC fiber and liquid-state twisted DSC wire, respectively. The DSCs were repeatedly heated to 70 °C and then cooled down to 20 °C. (e) Efficiency changes of a quasi-solid-state coaxial DSC fiber after heating from 20 to 120 °C and then cooling down to 20 °C. (f) Dependence of the efficiency on the cycle number for a typical quasi-solid-state coaxial DSC fiber that was heated to 120 °C and cooled down to 20 °C for 50 cycles.

For the coaxial photovoltaic fiber, the photovoltaic parameters of V_{oc}, J_{sc}, FF also remain almost unchanged under the different incident angles (Fig. 3c). Therefore, the energy conversion efficiencies are independent of the incident angle. These photovoltaic fibers can be stably and efficiently performed due to the use of the quasi-solid-state electrolyte. Fig. 3d has traced the changes of photovoltaic parameters of V_{oc}, J_{sc}, FF and η at a period of 300 hours in mimicking the typical use in air. All parameters remained unchanged in the measured time scale, and the energy conversion efficiencies varied by less than 5%.

These quasi-solid-state coaxial fiber-shaped DSCs exhibit a high flexibility. As shown in Fig. 4a and b, a photovoltaic fiber with a length of 2 cm can be bent to ~60° without breaking. No structural damage has been monitored by scanning electron microscopy either. The flexible property of the photovoltaic fiber has been further quantitatively studied by tracing the change of the energy conversion efficiency (Fig. 4c and S8†). The energy conversion efficiencies slightly decreased by less than 2% after bending for 20 cycles and less than 5% after 100 cycles as the coaxial structure is well maintained during bending. In contrast, for the conventional twisted DSC wire, the energy conversion efficiencies are decreased by higher than 25% and 30% after bending for 20 and 100 cycles, respectively (Fig. 4c). The reduced efficiencies in the twisted DSC wire result from the decreasing J_{sc}. The two fiber electrodes are peeled away from each other after bending for only 10 cycles (Fig. S9†), so the diffusion length for I^- ions is increased to slow the dye regeneration. Therefore, the photoelectrons may have more chances to recombine with I_3^- ions in the electrolyte, which reduces J_{sc}.[30]

The quasi-solid-state coaxial DSC also shows a high thermal stability. The energy conversion efficiency was traced in a heating and cooling cycle between 20 and 70 °C (Fig. 5a). The efficiencies are slightly increased with the increasing temperature below 40 °C and then slightly decreased with the further increase to 70 °C. The efficiencies varied by less than 10%

during the heating process. In addition, the efficiencies are well reverted upon cooling down to 20 °C, and they are varied by less than 6%. In contrast, the efficiency of the liquid-state twisted DSC drops by ~55% when the temperature is increased to above 70 °C and cannot be recovered after being cooled to 20 °C under the same conditions (Fig. 5b). To further investigate the long-term thermal stability, the quasi-solid-state coaxial DSC was repeatedly heated and cooled for 50 cycles (Fig. 5c), and the efficiency can be well maintained by ~93%. As a strong comparison, the efficiency of the liquid-state twisted DSC wire is maintained at ~46% after the first cycle and ~43% after the 50^{th} cycle (Fig. 5d). The quasi-solid-state coaxial DSC fiber exhibited a stable performance at a temperature as high as 120 °C (Fig. 5e). Fig. 5f further showed the efficiency change of an quasi-solid-state coaxial DSC fiber after heating and cooling for a series of cycles, and the efficiency was maintained at ~91% after 50 cycles.

In summary, a quasi-solid-state, coaxial DSC fiber, was firstly, to our best knowledge, developed with a high performance including a high thermal stability and flexibility that offer particularly promising applications for flexible devices at high temperatures. The novel photovoltaic fiber has also established some foundations for future photovoltaics and electronics with an ongoing push towards smaller and faster devices that are still confined to the planar silicon wafer.

Acknowledgements

This work was supported by NSFC (91027025, 21225417), MOST (2011CB932503, 2011DFA51330), STCSM (11520701400, 12nm0503200), Fok Ying Tong Education Foundation, and the Program for Professor of Special Appointment at Shanghai Institutions of Higher Learning.

References

1 A. Yella, H.-W. Lee, H. N. Tsao, C. Yi, A. K. Chandiran, M. K. Nazeeruddin, E. W.-G. Diau, C.-Y. Yeh, S. M. Zakeeruddin and M. Grätzel, *Science*, 2011, **334**, 629–634.
2 Z. Yang, T. Chen, R. He, G. Guan, H. Li and H. Peng, *Adv. Mater.*, 2011, **23**, 5636–5639.
3 Z. Yang, M. Liu, C. Zhang, W. W. Tjiu, T. Liu and H. Peng, *Angew. Chem., Int. Ed.*, 2013, **52**, 3996–3999.
4 Y. Xue, J. Liu, H. Chen, R. Wang, D. Li, J. Qu and L. Dai, *Angew. Chem., Int. Ed.*, 2012, **51**, 12124–12127.
5 W. Kwon, J.-M. Kim and S.-W. Rhee, *J. Mater. Chem. A*, 2013, **1**, 3202–3215.
6 L. Kavan, J.-H. Yum and M. Graetzel, *ACS Appl. Mater. Interfaces*, 2012, **4**, 6999–7006.
7 L. Kavan, J.-H. Yum and M. Graetzel, *Nano Lett.*, 2011, **11**, 5501–5506.
8 X. Yin, Z. Xue, L. Wang, Y. Cheng and B. Liu, *ACS Appl. Mater. Interfaces*, 2012, **4**, 1709–1715.
9 P. Zhang, C. Wu, Y. Han, T. Jin, B. Chi, J. Pu and L. Jian, *J. Am. Ceram. Soc.*, 2012, **95**, 1372–1377.
10 J.-Y. Liao, B.-X. Lei, H.-Y. Chen, D.-B. Kuang and C.-Y. Su, *Energy Environ. Sci.*, 2012, **5**, 5750–5757.
11 L. Zhang, E. Shi, C. Ji, Z. Li, P. Li, Y. Shang, Y. Li, J. Wei, K. Wang and H. Zhu, *Nanoscale*, 2012, **4**, 4954–4959.
12 T. Chen, L. Qiu, Z. Cai, F. Gong, Z. Yang, Z. Wang and H. Peng, *Nano Lett.*, 2012, **12**, 2568–2572.
13 S. Zhang, C. Ji, Z. Bian, R. Liu, X. Xia, D. Yun, L. Zhang, C. Huang and A. Cao, *Nano Lett.*, 2011, **11**, 3383–3387.
14 I. Chung, B. Lee, J. He, R. P. Chang and M. G. Kanatzidis, *Nature*, 2012, **485**, 486–489.
15 H. Wang, X. Zhang, F. Gong, G. Zhou and Z. S. Wang, *Adv. Mater.*, 2012, **24**, 121–124.
16 T. N. Peiris, S. Senthilarasu and K. U. Wijayantha, *J. Phys. Chem. C*, 2011, **116**, 1211–1218.
17 S. Zhang, C. Ji, Z. Bian, P. Yu, L. Zhang, D. Liu, E. Shi, Y. Shang, H. Peng and Q. Cheng, *ACS Nano*, 2012, **6**, 7191–7198.
18 T. Chen, L. Qiu, Z. Yang and H. Peng, *Chem. Soc. Rev.*, 2013, **42**, 5031–5041.
19 B. Weintraub, Y. Wei and Z. L. Wang, *Angew. Chem.*, 2009, **121**, 9143–9147.
20 J. Bae, Y. J. Park, M. Lee, S. N. Cha, Y. J. Choi, C. S. Lee, J. M. Kim and Z. L. Wang, *Adv. Mater.*, 2011, **23**, 3446–3449.
21 X. Sun, T. Chen, Z. Yang and H. Peng, *Acc. Chem. Res.*, 2012, **46**, 539–549.
22 (*a*) Y. Bai, Y. Cao, J. Zhang, M. Wang, R. Li, P. Wang, S. M. Zakeeruddin and M. Grätzel, *Nat. Mater.*, 2008, **7**, 626–630; (*b*) Y. Cao, J. Zhang, Y. Bai, R. Li, S. M. Zakeeruddin, M. Grätzel and P. Wang, *J. Phys. Chem. C*, 2008, **112**, 13775–13781.
23 C. Zhang, J. Dai, Z. Huo, X. Pan, L. Hu, F. Kong, Y. Huang, Y. Sui, X. Fang, K. Wang and S. Dai, *Electrochim. Acta*, 2008, **53**, 5503–5508.
24 (*a*) J. M. Macak, H. Tsuchiya and P. Schmuki, *Angew. Chem., Int. Ed.*, 2005, **44**, 2100–2102; (*b*) J. R. Jennings, A. Ghicov, L. M. Peter, P. Schmuki and A. B. Walker, *J. Am. Chem. Soc.*, 2008, **130**, 13364–13372; (*c*) H. Yang, W. Fan, A. Vaneski, A. S. Susha, W. Y. Teoh and A. L. Rogach, *Adv. Funct. Mater.*, 2012, **22**, 2821–2829.
25 X. Sun, W. Wang, L. Qiu, W. Guo, Y. Yu and H. Peng, *Angew. Chem., Int. Ed.*, 2012, **51**, 8520–8524.
26 M. R. Lee, R. D. Eckert, K. Forberich, G. Dennler, C. J. Brabec and R. A. Gaudiana, *Science*, 2009, **324**, 232–235.
27 T. Chen, L. Qiu, H. G. Kia, Z. Yang and H. Peng, *Adv. Mater.*, 2012, **24**, 4623–4628.
28 Y. Fu, Z. Lv, S. Hou, H. Wu, D. Wang, C. Zhang and D. Zou, *Adv. Energy Mater.*, 2012, **2**, 37–41.
29 L. Peter, *Acc. Chem. Res.*, 2009, **42**, 1839–1847.
30 A. Hagfeldt, G. Boschloo, L. Sun, L. Kloo and H. Pettersson, *Chem. Rev.*, 2010, **110**, 6595–6663.